Photonic band gaps from a stack of right- and left-hand chiral photonic crystal layers

A. H. Gevorgyan*

Department of Physics, Yerevan State University, 1, Al. Manookian St., Yerevan 0025, Armenia

(Received 15 October 2011; revised manuscript received 18 January 2012; published 21 February 2012)

In the present paper we investigated the optical properties of a stack of right- and left- hand chiral photonic crystal layers. The problem is solved by *Ambartsumian's layer addition modified method*. We investigated the reflection spectra peculiarities of this system and showed that in contrast to a single cholesteric liquid crystal (CLC) layer this system has multiple photonic band gaps (PBGs) (at light normal incidence). We showed that this system has unique polarization properties, particularly the eigenpolarizations (EPs) of the system are degenerated (i.e., the two EPs coincide) for an even number of layers and, in contrast to ordinary gyrotropic systems, the polarization plane rotation decreases if the system thickness is increased, the rotation sign depends on the first sublayer chirality sign, the system is very sensitive to the change of the sublayer number in the system, etc. We also investigated the influence of sublayer thicknesses, incidence angle, the sublayer local dielectric anisotropies, the sublayer helix pitches on the reflection peculiarities, and other optical parameters of the system.

DOI: 10.1103/PhysRevE.85.021704 PACS number(s): 42.70.Df, 42.70.Qs, 61.30.−v, 78.67.−n

I. INTRODUCTION

The current research and development in optical materials for photonic application are largely centered on structured materials that exhibit unique physical and optical properties [1–3]. In particular, photonic crystals (PCs) again draw a lot of attention due to their interesting physical properties and their relevance for development of new electro-optical and photonic devices. PCs exhibit photonic band gaps (PBGs), preventing light propagation in certain frequency ranges, which can be suitably tuned, just modifying their internal stacked structure [4–7]. As these structures are designed artificially or in a self-assembling manner, they can be prepared with substantially beforehand given properties, which lead to many challenging problems of theoretical and applied character. The optical devices constructed on the basis of PCs result in intelligent, multifunctional, and tunable optics, which possess such good traits as their compactness, small losses, high reliability, and compatibility with other devices. The PCs with tunable parameters are of special interest. The cholesteric liquid crystals (CLCs) are classic examples of PCs with easily tunable parameters. A CLC is a self-assembled photonic crystal formed by rod-like molecules, including chiral molecules that arrange themselves in a helical fashion. The CLC has a single PBG and an associated one-color reflection band for circularly polarized light with the same handedness as the CLC helix (at normal light incidence). The parameters of the CLCs can be easily tuned by external electrical or magnetic fields, or by thermal gradient, or IR radiation, etc. And a suitable manipulation of the CLCs layer parameters allows fine tuning of their PBG and other characteristics. On the other hand, recently PCs with multiple PBGs are of great interest. They find wide application, in particular, in the display industry.

The formation of multiple PBGs in one-dimensional stacked structures containing CLC layers and isotropic and anisotropic layers, as well as quasiperiodic systems characterized by Fibonacci numbers, has been reported theoretically and experimentally [8–14], and their investigations are still on-going. In Ref. [15] reflection peculiarities of the stack of two-layer CLC which differ from each other only by the helix sign was theoretically investigated. It is shown that this system makes it possible to obtain a 100% polarized diffraction reflection. The EPs of this system are degenerated. On the other hand, it was experimentally demonstrated that the introduction of photopolymerizable monomers into a cholesteric medium can generate regions with helicity inversion after ultraviolet (UV) light curing [16,17]. Such a polymer-cholesteric gel behaves as an infrared hyperreflective network that is almost independent on the light polarization. Reference [18] experimentally investigated novel hybrid structures composed of a dye-doped low-molecular-weight CLC sandwiched by multilayered polymer CLC films with right- and left-hand polymer CLC layers and evaluated their lasing characteristics. It was shown that lasing with an extremely reduced threshold can be observed.

A polarization-universal rejection filter based on periodically twisted nematic liquid crystal was proposed by Sarkissian *et al.* [19]. In this device, the nematic director does not rotate helicoidally around a fixed axis, as it does in CLC, but oscillates in the transverse plane, instead. In other words, the proposed PC is a structurally chiral material with a periodic transverse perturbation. The circularly polarized-discriminatory feature of a standard structurally chiral material is lost almost totally, and theoretical analysis showed that virtually identical PBGs are observed for both left and right circularly polarized plane waves. Reyes and Lakhtakia theoretically investigated the optical properties of structurally chiral material with periodic transverse perturbation such that its unit cell contains structurally left-handed and structurally right-handed halves that are otherwise identical [20]. They showed that this system exhibits an electrically tunable, polarization-universal band gap for normal incident plane wave.

In this work we investigate the reflection and polarization properties of the multilayered structure representing a stack of right- and left-hand chiral photonic crystal layers (Fig. 1). We found many new interesting peculiarities of this system, which also can have important applications.

*agevorgyan@ysu.am

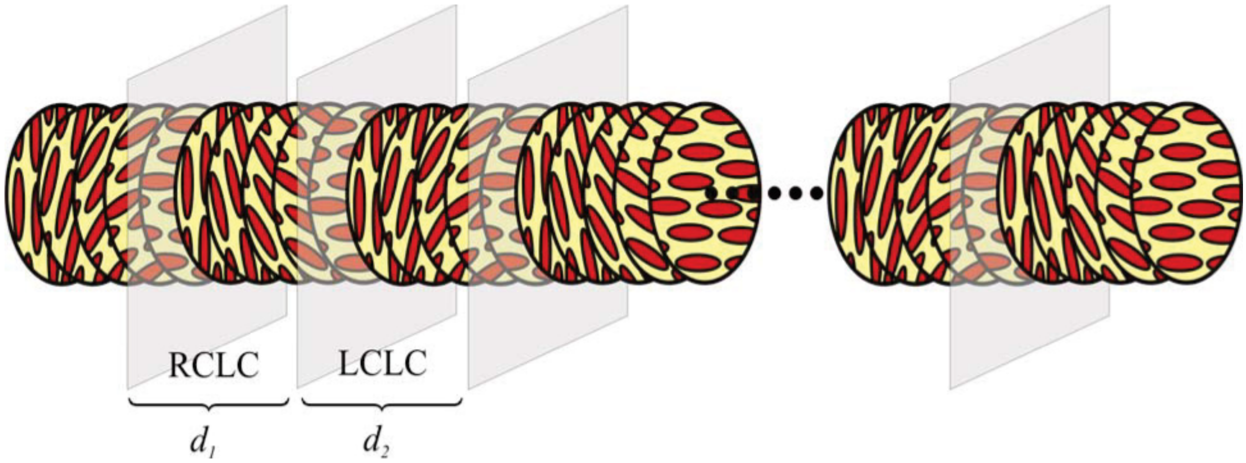

FIG. 1. (Color online) A sketch diagram of a model of a stack of right- and left-hand cholesteric liquid crystal layers.

The rest of the paper is organized as follows: In the following Sec. II we formulate the methodology and the basic principles for calculation of reflection and transmission matrices and EPs as well. In Sec. III we carry out the numerical calculations and analyze the reflection (transmission) and polarization plane rotation, polarization ellipticity, and EPs azimuth and ellipticity spectra peculiarities of the proposed system. The concluding remarks are given in Sec. IV.

II. THE METHOD OF THE ANALYSIS

The problem is solved by Ambartsumian's layer addition modified method adjusted to solution of such problems (see Refs. [14,15]).

According to *Ambartsumian's layer addition modified method,* if there is a system consisting of two adjacent (from left to right) layers, A and B, then the reflection transmission matrices of the system, $A+B$, viz. $\hat{R}_{A+B}$ and $\hat{T}_{A+B}$, are determined in terms of similar matrices of its component layers by the matrix equations

$$\begin{aligned} \hat{R}_{A+B} &= \hat{R}_A + \tilde{\hat{T}}_A \hat{R}_B [\hat{I} - \tilde{\hat{R}}_A \hat{R}_B]^{-1} \hat{T}_A, \\ \hat{T}_{A+B} &= \hat{T}_B [\hat{I} - \tilde{\hat{R}}_A \hat{R}_B]^{-1} \hat{T}_A, \end{aligned} \tag{1}$$

where $\hat{I}$ is the unit matrix, and the tilde denotes the corresponding reflection and transmission matrices for the reverse direction of light propagation. For instance, in the case when the layer of the medium is bordered on both sides by the same medium, the reflection and transmission matrices for the light incident from the left and from the right are connected with each other by the relations

$$\begin{aligned} \tilde{\hat{T}} &= \hat{F}^{-1} \hat{T} \hat{F}, \\ \tilde{\hat{R}} &= \hat{F}^{-1} \hat{R} \hat{F}, \end{aligned} \tag{2}$$

where $\hat{F} = \left(\begin{smallmatrix} 1 & 0 \\ 0 & -1 \end{smallmatrix}\right)$ for the linear base polarizations and $\hat{F} = \left(\begin{smallmatrix} 0 & 1 \\ 1 & 0 \end{smallmatrix}\right)$ for the circular base polarizations.

The exact reflection and transmission matrices for a finite *CLC layer* (at light normal incidence) are well known [21]. Let us present the solution of the boundary problem of light transmission through the single finite layer of CLC in the form

$$\vec{E}_r = \hat{R}\vec{E}_i, \quad \vec{E}_t = \hat{T}\vec{E}_i, \tag{3}$$

where the indices i, r, and t denote the incident, reflected, and transmitted waves fields, $\hat{R}$ and $\hat{T}$ are the reflection and transmission matrices, $\vec{E}_{i,r,t} = E^{+}_{i,r,t}\vec{n}_+ + E^{-}_{i,r,t}\vec{n}_- = \left[\begin{smallmatrix} E^{+}_{i,r,t} \\ E^{-}_{i,r,t} \end{smallmatrix}\right]$, $\vec{n}_\pm = (\vec{x} \pm i\vec{y})/\sqrt{2}$, and we also have for the matrices $\hat{R}$ and $\hat{T}$ (according to [21,22]):

$$\begin{aligned} &R_{11} = R_{22} = H, \quad R_{12} = Q + iF, \quad R_{21} = Q - iF, \\ &T_{11} = (S - iN)\exp(i2ad), \quad T_{12} = V\exp(i2ad), \\ &T_{21} = V\exp(-i2ad), \quad T_{22} = (S + iN)\exp(-i2ad), \end{aligned} \tag{4}$$

where $H = \{\chi^2 r_2 r_1(c_1c_2 - 1) + 2u^2[r_2r_1(2\chi^2 m_1 - \gamma^2) - \alpha^2\delta^2\gamma^2]s_1s_2 - iu\sqrt{\alpha}\gamma(p_1s_1c_2 + p_2s_2c_1)\}/\Delta$, $F = \delta\chi\sqrt{\alpha}\{-2u\gamma\sqrt{\alpha}(s_1c_2 - s_2c_1) - i[r_2(c_1c_2 - 1) + 4u^2(m_1r_2 + \alpha\gamma^2)s_1s_2\}/\Delta$, $Q = u\gamma\delta\sqrt{\alpha}[4u\sqrt{\alpha}\gamma s_1s_2 + i(g_1s_2c_1 - g_2s_1c_2)]/\Delta$, $S = \gamma\sqrt{\alpha}[\gamma\sqrt{\alpha}(c_1 + c_2) - iu(b_1s_1 + b_2s_2)]/\Delta$, $V = \gamma\sqrt{\alpha}\delta\,[\sqrt{\alpha}(c_2 - c_1) - iu(q_2s_2 - q_1s_1)]/\Delta$, $N = \gamma\sqrt{\alpha}\chi[ir_1(c_2 - c_1) - 2u\sqrt{\alpha}(l_1s_1 + l_2s_2)]/\Delta$, $\Delta = -\chi^2 {r_2}^2 + (\chi^2 {r_2}^2 + 2\alpha\gamma^2)c_1c_2 + 2u^2[\alpha^2\delta^2\gamma^2 - {r_1}^2(2\chi^2 m_2 + \delta^2) + 4\alpha\chi^2(\delta^2 - 2m_2)]s_1s_2 - 2ui\gamma\sqrt{\alpha}(b_1s_1c_2 + b_2s_2c_1)$, $b_{1,2} = r_1w_{1,2} \pm \alpha\delta^2$, $p_{1,2} = r_2w_{1,2} \mp \alpha\delta^2$, $q_{1,2} = r_1 \pm \alpha\gamma$, $g_{1,2} = r_2 \pm \alpha\gamma$, $w_{1,2} = \gamma \pm 2\chi^2$, $l_{1,2} = \gamma \pm 2$, $r_{1,2} = 1 \pm \alpha$, $s_{1,2} = \sin(k_{1,2}d)/(k_{1,2}d)$, $c_{1,2} = \cos(k_{1,2}d)$, $k_{1,2} = 2ub^{\pm}/d$, $b^{\pm} = \sqrt{1 + \chi^2 - \delta \pm \gamma}$, $\gamma = \sqrt{4\chi^2 + \delta^2}$, $\alpha\ \sqrt{\varepsilon_m/\varepsilon}$, ε is the dielectric permittivity of the surrounding of the CLC layer, $u = \pi d\sqrt{\varepsilon_m}/\lambda$, d is CLC layer thickness, $a = 2\pi/p$, p is the helix pitch, $\chi = \lambda/(p\sqrt{\varepsilon_m})$, λ is the wavelength in vacuum, $\varepsilon_m = (\varepsilon_1 + \varepsilon_2)/2$, $\delta = (\varepsilon_1 - \varepsilon_2)/(\varepsilon_1 + \varepsilon_2)$, ε_1, ε_2 are the principal values of the local dielectric permittivity tensor.

Matrices $\hat{R}$ and $\hat{T}$ for the CLC layer are essentially simplified for $\alpha = 1$. For this case we have

$$\begin{aligned} R_{jj} &= iu\delta^2(s_1a_2 - s_2a_1)/\Delta, \\ R_{jk} &= iu\delta(h_ks_1a_2 + h_js_2a_1)/\Delta, \\ T_{jj} &= \exp(-\eta_j ad)(h_ja_2 + h_ka_1)/\Delta, \\ T_{jk} &= -\delta\exp(-\eta_j ad)(a_1 - a_2)/\Delta, \\ \Delta &= 2\gamma a_1a_2, \quad a_{1,2} = c_{1,2} \mp iul_{1,2}s_{1,2}, \end{aligned}$$

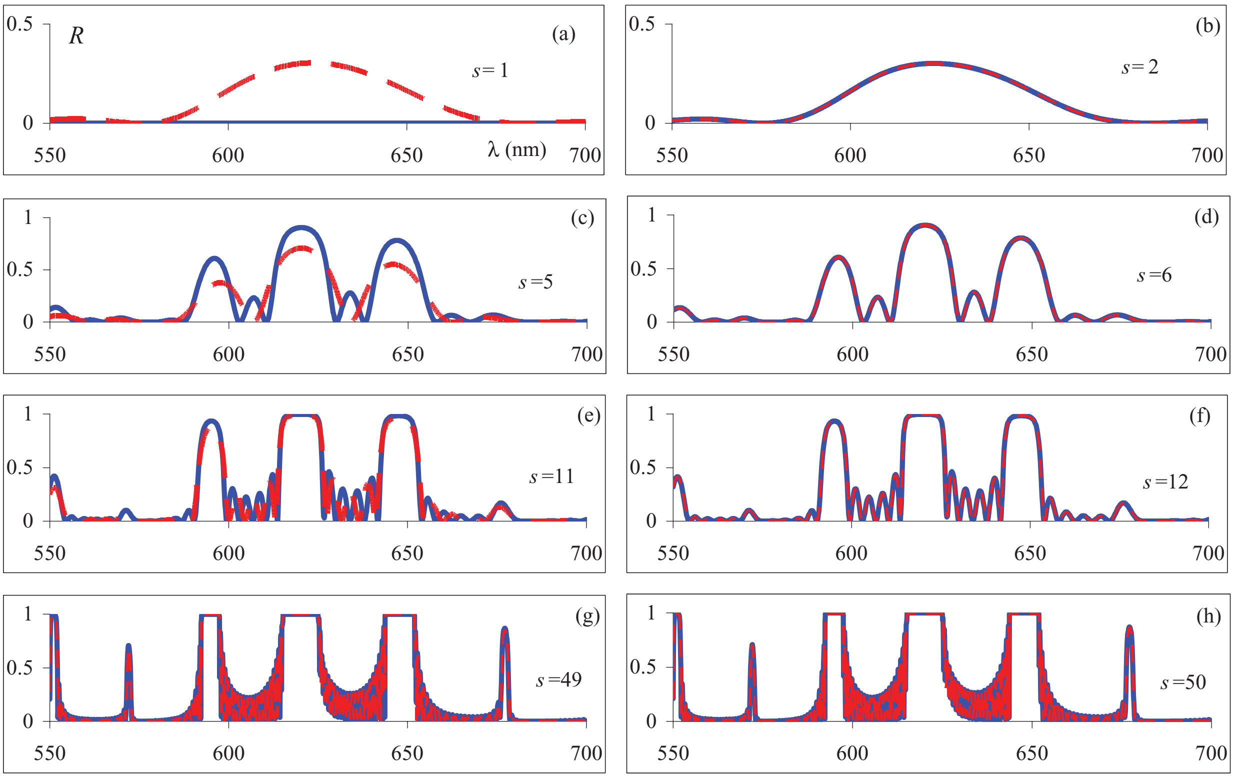

FIG. 2. (Color online) The reflection spectra for various numbers of sublayers s. The incident light has RCP [the red (light gray) dashed lines] and LCP [the blue (dark gray) solid lines]. $d_1 = d_2 = 2500$ nm, $\alpha = 1$.

$$h_{1,2} = \gamma \pm 2\chi, \quad \eta_k = (-1)^k, j,k = 1,2. \tag{5}$$

We carried out the calculations of transmission (reflection) through the stack of right- and left- hand CLC layers on the base of matrix equations (1), applying them in turn as we were adding a new CLC layer to the stack, which was considered as the "A" layer and the new added one was considered as the layer "B." Therefore, to organize the calculations well system Eq. (1) was presented in the form of the system of the following difference matrix equations:

$$\begin{aligned} \hat{R}_j &= \hat{r}_j + \tilde{\hat{t}}_j \hat{R}_{j-1}(\hat{I} - \tilde{\hat{r}}_j \hat{R}_{j-1})^{-1}\hat{t}_j, \\ \hat{T}_j &= \hat{T}_{j-1}(\hat{I} - \tilde{\hat{r}}_j \hat{R}_{j-1})^{-1}\hat{t}_j, \end{aligned} \tag{6}$$

with $\hat{R}_0 = \hat{0}$ and $\hat{T}_0 = \hat{I}$. Here $\hat{R}_j, \hat{T}_j, \hat{R}_{j-1}$ and $\hat{T}_{j-1}$ are the reflection and transmission matrices for the system consisting of the jth and $(j-1)$th sublayers, respectively; and $\hat{r}_j, \hat{t}_j$ are the reflection and transmission matrices for the jth sublayer; $\hat{0}$ is the zero matrix.

Let us note that there are many methods of solving the light propagating problem through a system containing anisotropic, gyrotropic, liquid crystalline, etc layers (see below.) Here it is convenient to apply Ambartsumian's layer addition modified method because the exact reflection and transmission matrices of the finite CLC layer are known.

Let us now consider the EPs. The EPs are the two polarizations of the incident light which do not change when light transmits through the system [14,23]. The EPs and eigenvalues

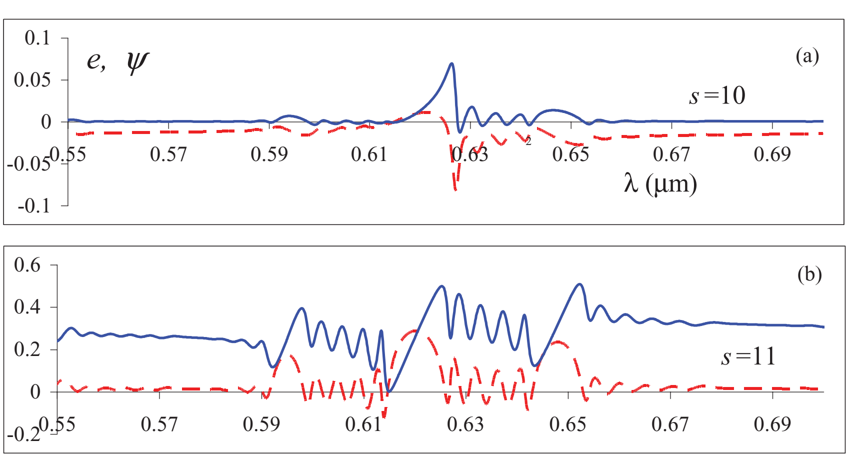

FIG. 3. (Color online) The polarization plane rotation spectra [ψ, the blue (dark gray) solid lines] and the polarization ellipticity spectra [e, the red (light gray) dashed lines] for various numbers of sublayers s. The incident light is linearly polarized. $d_1 = d_2 = 2500$ nm, $\alpha = 1$.

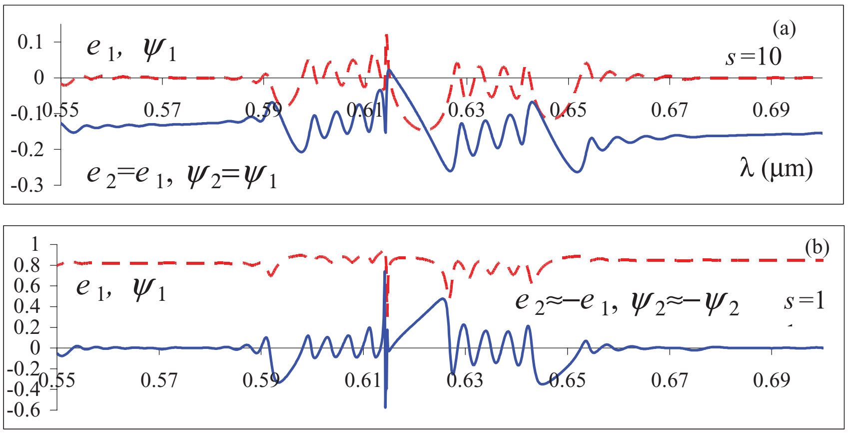

FIG. 4. (Color online) The ellipticity spectra [e_1, the red (light gray) dashed lines] and azimuth [ψ_1, the blue (dark gray) solid lines] of the first EP for various numbers of sublayers s. $d_1 = d_2 = 2500$ nm, $\alpha = 1$.

(the amplitude transmission and reflection coefficients for the incident light with EPs) deliver much information about the peculiarities of light interaction with the system. Therefore, the calculation of EPs and eigenvalues of every optical device is important. It follows from the definition of the EP that they must be connected with the polarizations of the excited internal waves (the eigenmodes) aroused in the medium. (In the majority of cases they coincide with the polarizations of the eigenmodes). Naturally there are certain differences in the general case: there exist only two EPs; meanwhile, the number of eigenmodes can be more than two, and the polarizations of these modes can differ from each other (for the nonreciprocity media, for instance).

The EPs automatically take the influence of the dielectric borders into account. As it is known (in particular, for normal incidence) the EPs of either CLC or gyrotropic media practically coincide with the orthogonal circular polarizations; meanwhile, they coincide with the orthogonal linear polarizations for the nongyrotropic media. It follows from the above that investigation of the EPs peculiarities is especially

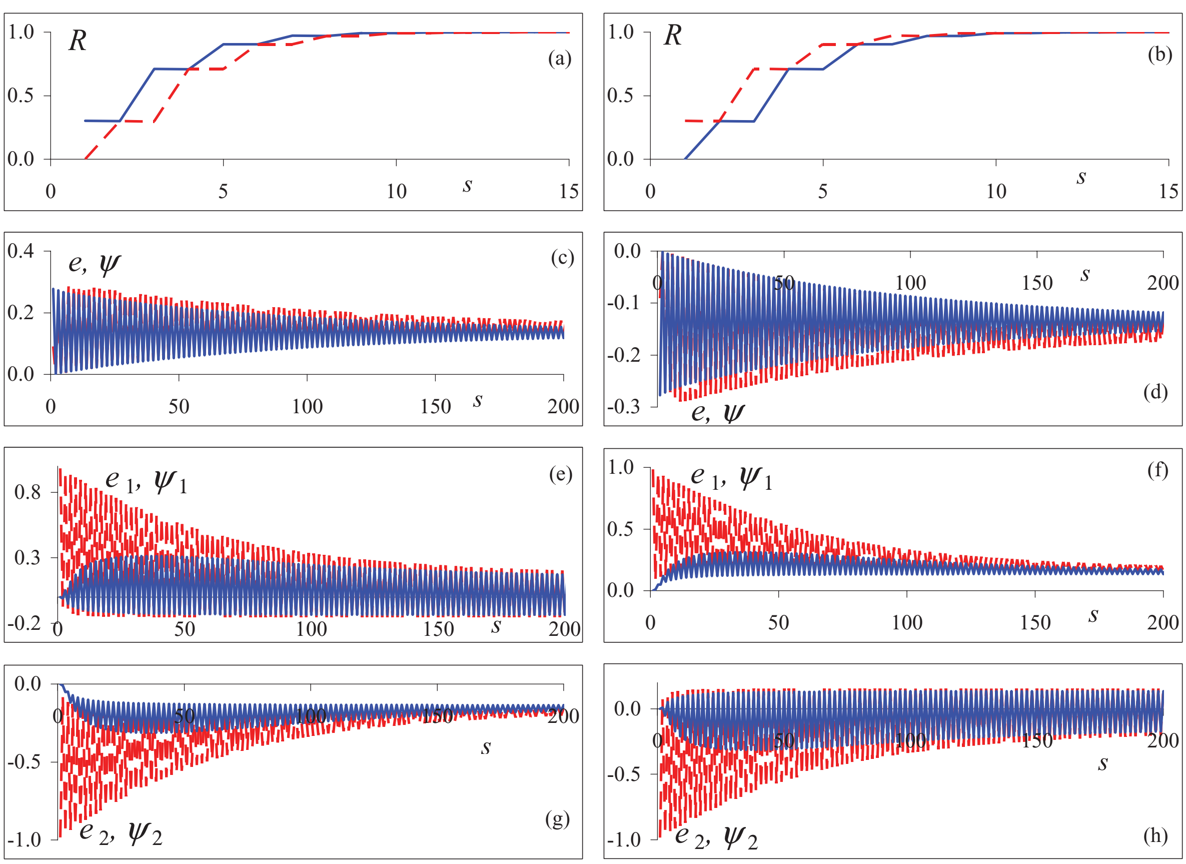

FIG. 5. (Color online) The dependence of the reflection R (a), (b) for the RCP light [the red (light gray) dashed line] and the light with the LCP [the blue (dark gray) solid line], polarization plane rotation ψ (blue line), polarization ellipticity e (the red line, c and d), ellipticities $e_{1,2}$ [the red (light gray) dashed lines], and azimuths $\psi_{1,2}$ [the blue (dark gray) solid lines] of the EPs (e, f, g and h), on the sublayer number s for the case when the first sublayer has the right helix (a, c, e and g) and when it has the left helix (b, d, f and h). λ = 620 nm, $d_1 = d_2 = 2500$ nm.

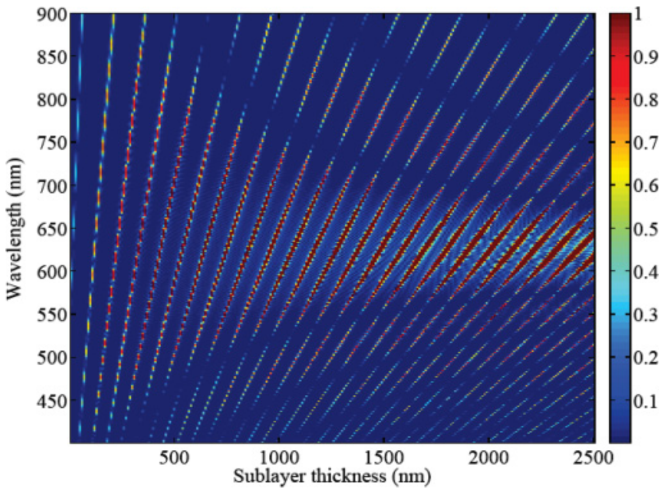

FIG. 6. (Color online) The density plot of the reflection spectra as a function of the sublayer thicknesses $d = d_1 = d_2$. The incident light is of the RCP. $\alpha = 1$, $s = 50$.

important for the case of inhomogeneous media for which the exact solution of the problem is unknown.

Denoting the ratio of the complex field components by $\chi_i = E_i^-/E_i^+$ for the incidence wave at the entrance of the system, and the same ratio at the exit by $\chi_t = E_t^-/E_t^+$, and taking into account that

$$\begin{bmatrix} E_t^+ \\ E_t^- \end{bmatrix} = \begin{bmatrix} T_{11} & T_{12} \\ T_{21} & T_{22} \end{bmatrix} \begin{bmatrix} E_i^+ \\ E_i^- \end{bmatrix},$$

we find that

$$\chi_t = (T_{22}\chi_i + T_{21})/(T_{12}\chi_i + T_{11}), \tag{7}$$

where T_{ij} are the elements of the total system transmission matrix.

The function $\chi_t = f(\chi_i)$ is called *polarization transfer function* [23] and it bears information about polarization ellipse transformation when light is transmitted through the system. Every optical system has two EPs, which are obtained through substitution χ_t from Eq. (2) into the equation $\chi_i = \chi_t$. Thus we get

$$\chi_{1,2} = \frac{T_{22} - T_{11} \pm \sqrt{(T_{22} - T_{11})^2 + 4T_{12}T_{21}}}{2T_{12}}. \tag{8}$$

The ellipticities $e_{1,2}$ and the azimuths $\psi_{1,2}$ of the EPs are expressed by $\chi_{1,2}$ through the following formulas

$$\psi_{1,2} = -\frac{1}{2}\arg(\chi_{1,2}), \quad e_{1,2} = \operatorname{arctg}\left(\frac{|\chi_{1,2}| - 1}{|\chi_{1,2}| + 1}\right). \tag{9}$$

III. RESULTS AND DISCUSSION

We analyzed the spectral properties of the multilayered structure of right- and left-hand chiral photonic crystal layers as presented in Fig. 1. The ordinary and extraordinary refractive indices of CLC sublayers were taken to be $n_o = 1.4639$ and $n_e = 1.5133$ (and these are the parameters of the *CLC* cholesteryl-nonanoate : cholesteryl-chloride : cholesteryl-acetate (20:15:6) composition, at the temperature $t = 25\,^{\circ}$C). The *CLC sublayers* helixes are right and left handed and their

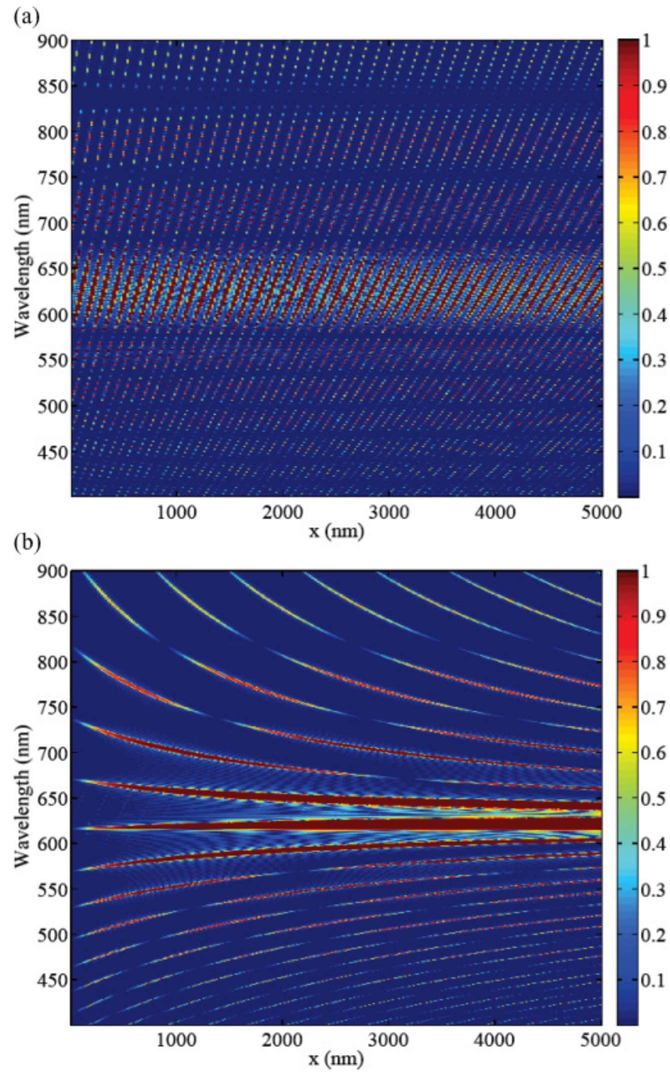

FIG. 7. (Color online) The density plot of the reflection spectra as a function of the sublayer thicknesses $d_2 = x$. The incident light has the (a) right and (b) left circular polarization. $d_1 = 2500$ nm, $s = 50$, $\alpha = 1$.

pitches are $p_{1,2} = \pm 420$ nm. So the incident onto a single *CLC layer* with, for instance, right helix, light with the right circular polarization (RCP) has a PBG, and the light with the left circular polarization (LCP) has not.

From the experimental point of view, fabricating a stack of right- and left-hand chiral photonic crystal layers can be carried out on the base of polymerized CLCs, as it was done, for instance, in Ref. [18]. Besides, as it was experimentally shown in Refs. [16,17], the introduction of photopolymerizable monomers into a cholesteric medium can generate regions with helicity inversion after UV light curing.

Below we investigate the effects of number of sublayers in the system on the reflection spectra and on the spectra of polarization characteristics.

A. Reflection spectra: Spectra of polarization characteristics

Here we investigate the case when the sublayers of the two types have the same parameters and differ from each other by the helicity sign only. In Fig. 2 we present the reflection

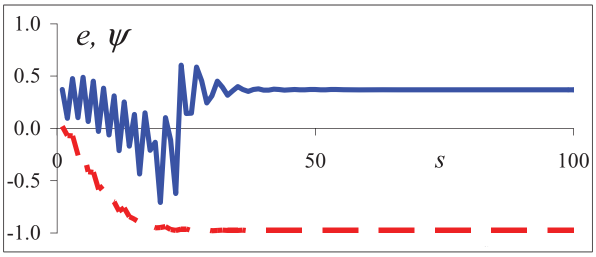

FIG. 8. (Color online) Polarization plane rotation dependencies [ψ, the blue (dark gray) solid lines] and polarization ellipticity dependences [e, the red (light gray) dashed lines] on the sublayer number s. The incident light is linearly polarized. $\lambda = 620$ nm, $d_1 = 2500$ nm, $d_1 = 500$ nm, $\alpha = 1$.

spectra for various sublayer numbers of the system, in the case of normal light incidence. The incident light has RCP [the red (light gray) dashed lines] and LCP [the blue (dark gray) solid lines]. Here and elsewhere we consider the case $\alpha = 1$, that is, we take the dielectric permittivity of the surrounding of the system ε to be equal to the average dielectric permittivity ε_m of each CLC sublayer.

As it is seen from Fig. 2, in contrast to a single CLC layer this system has multiple PBGs (at normal light incidence). (Let us note that at oblique light incidence the multiple PBGs have the single CLC layer, too [24].) At the zero order reflection the system manifests itself with three diffraction reflection peaks (red-green-blue reflection). This system does not manifest selectivity with respect to the incident wave polarization if the sublayer number of the system is even. On the contrary, if the said number is odd, the system manifests strong selectivity with respect to the incident wave polarization, particularly with the circular polarization (the reflection spectra of the orthogonal linear polarizations practically coincide). The difference of the orthogonal circular polarizations in the incident wave reflection in the PBGs vanishes if the sublayer number in the system increases. The diffraction efficiency of the other reflection orders also increases if the sublayer number increases.

Let us move to the polarization characteristics. Figure 3 presents the polarization plane rotation spectra [ψ, the blue (dark gray) solid lines] and the spectra of the polarization ellipticity [e, the red (light gray) dashed lines] for various sublayer numbers s for the normal wave incidence. The incident light is linearly polarized. Comparison of rotation curves for various sublayer numbers shows that the rotation in the system is by two orders higher for an odd number of sublayers than that for the sublayer even number, which could be expected. Let us note that for an even sublayer number the polarization plane rotation is not zero and it significantly differs from zero in the PBG. This is stipulated not only by diffraction multireflections from the each border of each sublayer, but also by dependencies of reflection and transmission (etc.) in each sublayer on the azimuth and polarization ellipticity of the incident light.

Figure 4 presents the spectra of the ellipticity [e_1, the red (light gray) dashed lines] and azimuth [ψ_1, the blue (dark gray) solid lines] of the first EP for various sublayer numbers s in the system for the normal incidence of light. If the sublayer number is even, the EPs are degenerated (both EPs coincide); if the sublayer number is odd, the EPs are quasicircular polarizations, which are quasiorthogonal outside the PBG.

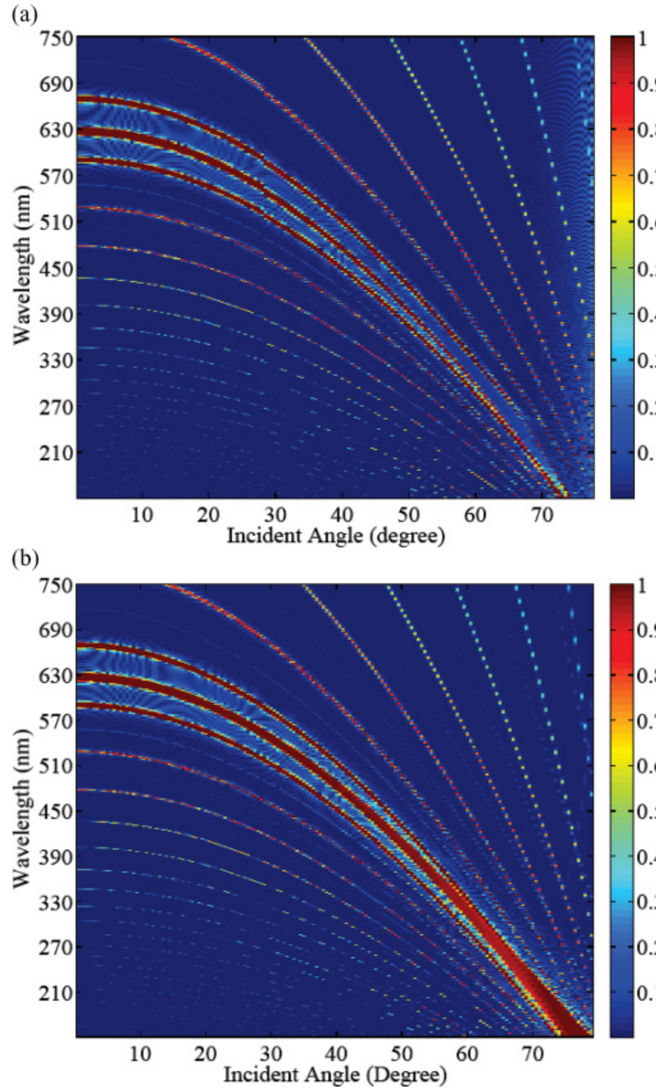

FIG. 9. (Color online) The density plot of the reflection spectra as a function of the incident angle are presented. The incident light is linearly polarized along the axes (a) x and (b) y. $s = 50$, $\alpha = 1$.

Let us note that significant changes of rotation of polarization plane and polarization azimuth, as well as of the EPs, take place in the PBGs, meanwhile, these changes have oscillating character with essentially small amplitudes elsewhere.

The essential peculiarity of the subject system are strong dependencies (especially the polarization ones) of its optical characteristics on the system sublayer number and the helicity character of the first sublayer (i.e., whether its helix is a right hand or left hand one). Figure 5 presents the dependencies of the reflection R (a, b) for the RCP light [the red (light gray) dashed line] and the light with LCP [the blue (dark gray) solid line], and those of the polarization plane rotation ψ [the blue (dark gray) solid line] and of polarization ellipticity e [the red (light gray) dashed line; c and d], and of ellipticities $e_{1,2}$ [the red (light gray) dashed lines] and of azimuths $\psi_{1,2}$ [the blue (dark gray) solid lines] of the EPs (e, f, g, h) on the system sublayer number s for the case when the first sublayer has a right-hand

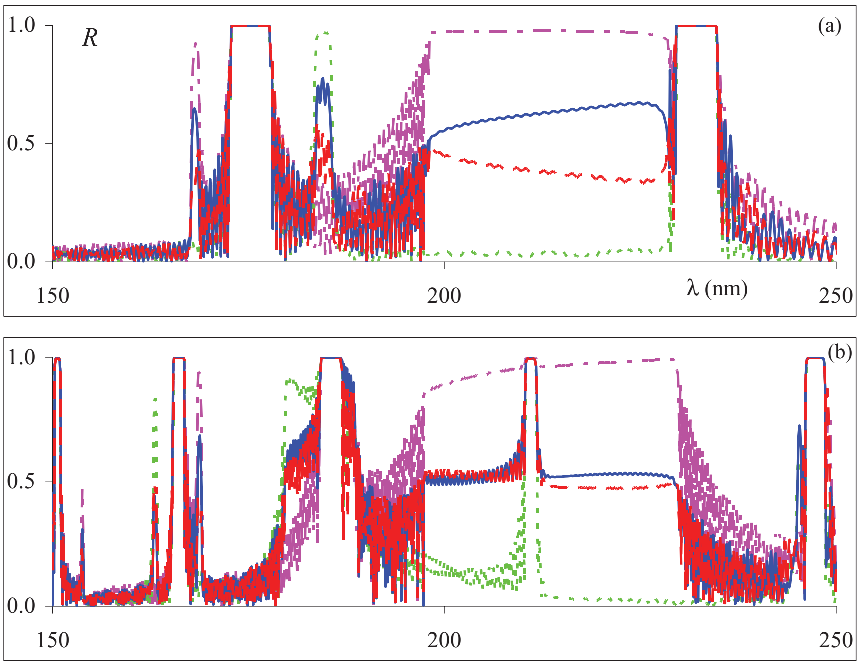

FIG. 10. (Color online) The reflection spectra for the oblique incidence (the incidence angle is$\vartheta = 70^{\circ}$). (a) $d_{1,2} = 2|p_{1,2}|$ and (b) $d_{1,2} = 4|p_{1,2}|$. The incident light is of the RCP [the red (dark gray) dashed lines] and LCP [the blue (darker gray) solid lines] and is linearly polarized along the axes x [the green (lighter gray) dash and dot lines] and y [the pink (light gray) dotted lines]. $|p_1| = |p_2|$. $s = 51$. $\alpha = 1$.

helicity (a, c, e, g), and when it has a left-hand helicity (b, d, f, h). First we have to note that in contrast to the amplitude characteristics, which practically lose their sensitivity both to the change of the sublayer number and helicity character of the first sublayer in the system, still for $s \geqslant 15$ the polarization characteristics practically do not lose this sensitivity. If the sublayer number increases, these characteristics are changed with jumps with slowly changing amplitudes. Such a system is particularly unique, for the sign of its polarization plane rotation depends on the helicity sign of the first sublayer (for the even sublayer number, too) and, besides, in contrast to the ordinary gyrotropic media, the polarization plane rotation magnitude decreases with oscillations if the system thickness increases. If the system thickness increases, the EPs turn into quasilinear polarizations (for a small thickness they are quasicircular, naturally, for an odd number of sublayers in the system, as mentioned above).

B. Impact of sublayers thicknesses

Now we move to the consideration of the influence of the sublayer thickness changes on the reflection spectra. First, let us consider (as above) the case when the sublayers of the two types have the same parameters but different helicity signs. Figure 6 presents the density plot of the reflection spectra as a function of the sublayer thicknesses $d = d_1 = d_2$. As the sublayer thicknesses increase, the diffraction efficiency in the PBGs increases, too, and the PBGs shift to the long wave region, and new PBGs appear, as well as an additional modulation is observed.

Now we consider the case when d_1 is fixed and only $d_2 = x$ changes. In Fig. 7 the density plot of the reflection spectra as a function of the sublayer thicknesses $d_2 = x$ are presented. The incident light has (a) right-hand and (b) left-hand circular polarizations. If$d_1 \neq d_2$, the properties of the system essentially differ from those for $d_1 = d_2$. First, the EPs (independent of sublayer number and helicity of the first sublayer) become circular basis polarizations (some weak differences of the EPs from ± 1 are observed in the PBGs). The system manifests stronger selectivity for the incident wave polarizations. In this case, the reflection spectra characteristic changes (depending on the changes of x) for the right-hand circularly polarized incident light essentially differ from those for the left-hand circularly polarized incident light, if the reflection spectra change regularities for the right-hand circularly polarized incident light practically do not change when x increases. Meanwhile, for the left-hand circularly polarized incident light, a significant frequency widening of the principal (i.e., red, green, blue) PBGs takes place. Moreover, the frequency locations of the PBGs (except the central one) are changed.

As our calculations show, in this case ($d_1 \neq d_2$), if the sublayer number increases, the optical (as well as the polarization) characteristics of the system reach a certain regime faster than those for $d_1 = d_2$(and after this the changes of these parameters are not observed when we add new sublayers). To demonstrate this we present the dependence of polarization plane rotation ψ [the blue (dark gray) solid lines] and polarization ellipticity e [the red (light gray) dashed lines] on the sublayer number for$d_1 \neq d_2$ (Fig. 8). The incident light is linearly polarized.

C. Oblique incidence

Now we move to the investigation of oblique light incidence. This problem of light propagation through the CLC layer was solved by different methods. Rokushima and Yamakita [25] and Wang and Lakhtakia [26] exemplify the use of the coupled-wave method, Abdulhalim *et al.* exemplify the use of the Berreman method [27], Ambartsumian's layer addition modified method is used in [28], Belyakov and Dimitrienko provided an approximate analytical method [29,30], Lakhtakia and Weiglhofer provided an exact analytical method [31], and Polo and Lakhtakia compared the exact analytical method with Berreman's method [32].

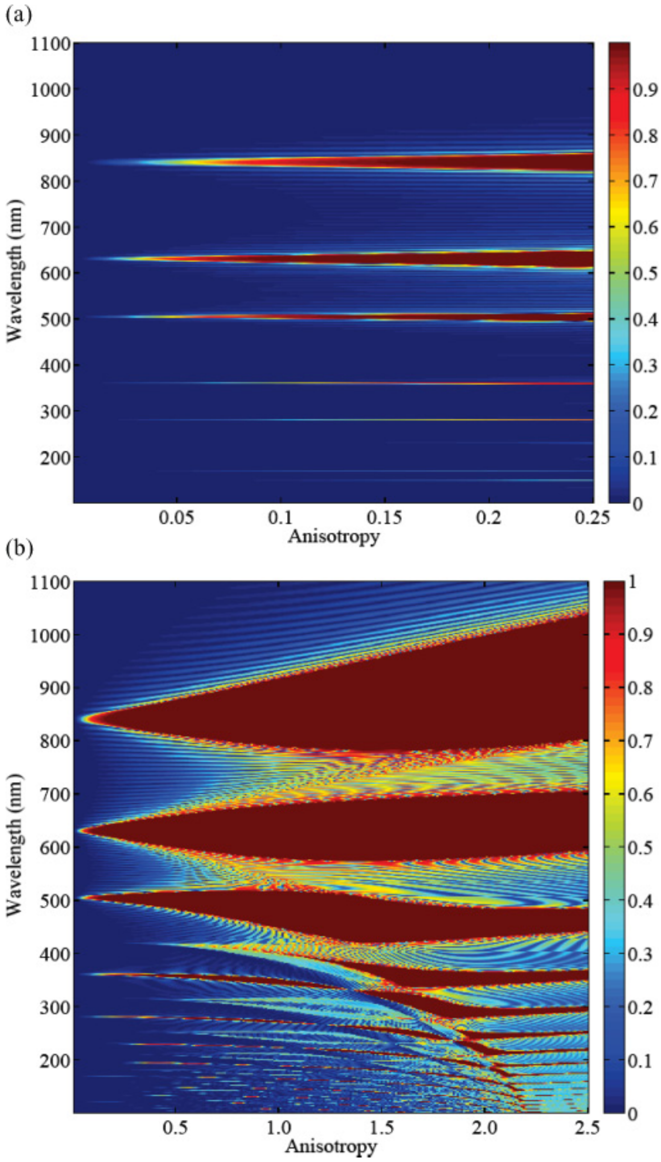

FIG. 11. (Color online) The density plot of the reflection spectra as a function of the anisotropy Δ. The incident light is of the RCP. $s = 50$, $d_1 = d_2 = 420$ nm, $\alpha = 1$.

We do the numerical calculations as follows. First we find the reflection and transmission matrices for each CLC sublayer. To do this we divide each CLC sublayer (with thicknesses $d_{1,2}$) into many thin layers of thicknesses, l_1, l_2, $l_3, \ldots, l_N$. If their maximum thickness is sufficiently small, one can consider that each "sub-sub-layer" is a linear birefringent plate, and the CLC sublayers with thicknesses $d_{1,2}$ can be considered as stacks of parallel and very thin birefringent layers, and that the principal axis of each sub-sub-layer is turned by the small angle $2\pi/N$ with respect to the preceding one. We find out the reflection and transmission matrices of each sublayer through the system of difference matrix equations (6), where $\hat{R}_j, \hat{T}_j, \hat{R}_{j-1}, \hat{T}_{j-1}$ are the reflection and transmission matrices of the jth and $(j-1)$th sub-sub-layers, respectively, and $\hat{r}_j, \hat{t}_j$ are the reflection and transmission matrices of the jth birefringent sub-sub-layer. Then to calculate the reflection or transmission of the whole system we again apply the system of difference matrix equations (6), but now $\hat{R}_j, \hat{T}_j, \hat{R}_{j-1}$ and $\hat{T}_{j-1}$ are the reflection and transmission matrices for the system consisting of j and $j-1$ CLC sublayers, respectively; and $\hat{r}_j, \hat{t}_j$ are the reflection and transmission matrices for the jth CLC sublayer. Thus, this problem is reduced to calculation of the reflection and transmission matrices of the birefringent homogeneous layer. The analytic solution of this problem is well known (see, for instance, [33]). We move to the analysis of the obtained results.

Figure 9 presents the density plot of the reflection spectra as a function of the incident angle. The incident light has linear polarizations along the axes x [Fig. 9(a)] and y [Fig. 9(b)]. The system does not manifest selectivity of polarization for small incidence angles (especially in the PBG), but it does if the incidence angle increases. For larger incidence angles, particularly strong selectivity appears with respect to the orthogonal linear polarizations (the selectivity is much smaller to the circular polarizations). For larger incidence angles, a two-, or three-, or more peak diffraction regions appear (the number of peaks mainly depends on the sublayer thicknesses) together with a total reflection region and a selective reflection region. These regions, depending on the incidence angle and the medium parameters, either are adjoined to each other, or they are separate. Such phenomena are also observed for the higher order diffraction reflections, too. If the incidence angle increases, the diffraction reflection region is shifted to the short wave region. For the larger incidence angles, diffraction reflections of the higher orders with significant intensity are excited, too, but their region widths are much narrower.

Figure 10 presents reflection spectra for the oblique incidence (the incidence angle, $\vartheta = 70^\circ$). Figure 10(a) presents the case when $d_{1,2} = 2|p_{1,2}|$, and Fig. 10(b) corresponds to the case when $d_{1,2} = 4|p_{1,2}|$ ($|p_1| = |p_2|$). The incident light has the RCP [the red (dark gray) dashed lines], and LCP [the blue (darker gray) solid lines], and it is linearly polarized along the axes x [the green (lighter gray) dash and dot lines] and y [the pink (light gray) dotted lines].

The investigation of the EPs peculiarities for the oblique incidence shows that the EP ellipticity magnitudes are mainly decreased for larger incidence angles.

D. Effects of local dielectric anisotropy

The dielectric anisotropy $\Delta = \frac{\varepsilon_1 - \varepsilon_2}{2}$ for the ordinary CLCs is of order 0.5 and smaller. But recently artificial crystals (metamaterials) are made, which have a dielectric anisotropy that can be varied in a large interval. It seems that helical periodic media like CLCs having huge local anisotropy can be created on their base. Such media with comparatively weak anisotropy have been created long ago [34,35]. On the other hand, recently the interest for the CLC enriched with nanoparticles has been increased (see [36], and references cited therein). The presence of nanoparticles (either ferroelectric or ferromagnetic) in the CLC structure leads to an essential increase of its local (both dielectric and magnetic) anisotropy, a significant change of the isotropic phase-liquid crystalline phase transition temperature, a significant change of the photonic band gap frequency width and the frequency localization, a change of the CLC elasticity coefficients, a significant increase of the CLC tuning possibilities, etc.

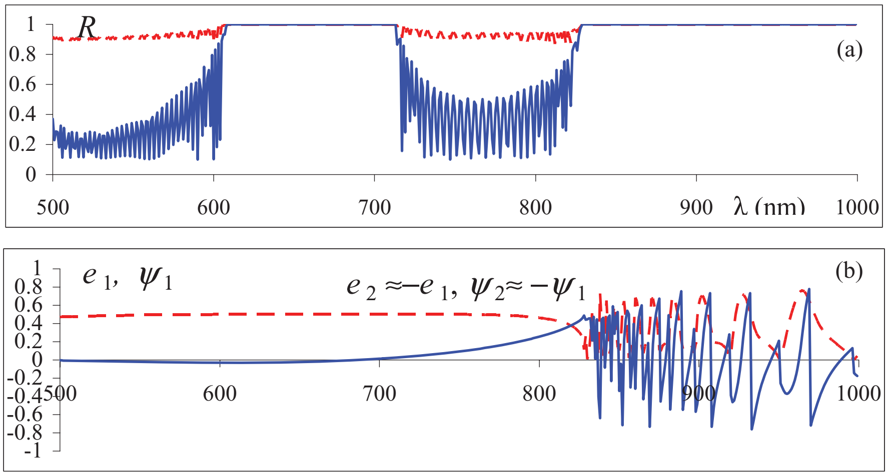

FIG. 12. (Color online) (a) The reflection spectra R. (b) The ellipticity spectra e_1 [the red (light gray) dashed line] and the azimuth spectra ψ_1 [blue (dark gray) solid line] of the first EPs. $\Delta = 3.0$, $s = 51$, $d_1 = d_2 = 2500$ nm, $\alpha = 1$.

It follows from the above that investigations of the optical peculiarities of a stack of right- and left-handed chiral photonic crystal layers for various values of its local dielectric anisotropy can have great interest. Representing the principal values of the dielectric permittivity tensor of the right- and left-handed CLC sublayers in the form $\varepsilon_1 = \varepsilon_0 + \Delta$ and $\varepsilon_2 = \varepsilon_0 - \Delta$, we investigate the influence of the anisotropy Δ on the reflection spectra. Figure 11 presents the density plot of the reflection spectra as a function of the anisotropyΔ. The incident light has right circular polarization. Figure 11(a) presents the case when the anisotropyΔ changes from 0 to 0.25, and Fig. 11(b) corresponds to the case of far larger interval (from 0 to 2.5). If the local anisotropy increases, the number of PBGs as well as their frequency positions and frequency widths increase, too. For larger anisotropies, the frequency widths of some PBGs begin to decrease and they even vanish. The selectivity of the incident wave polarizations appears (including the selectivity of the circular polarizations). The reflection outside the PBG increases. To demonstrate the appeared strong polarization selectivity of the incident wave we presented the reflection spectra for a large local dielectric anisotropy in Fig. 12(a). The incident light has the RCP [the red (light gray) dashed lines] and LCP [the blue (dark gray) solid lines]. As it is seen from the figure, if the reflections of the two circular polarizations coincide in the PBG, then on the contrary they strongly differ outside the PBG. Figure 12(b) presents the ellipticity spectra [e_1, the red (light gray) dashed lines] and the azimuth spectra [ψ_1, the blue (dark gray) solid lines] of the first EP for a large local dielectric anisotropy (for an odd number of sublayers in the system). As it is seen from this figure, the EPs for this large anisotropy stop being quasicircular; they are elliptical. Let us note that if the anisotropy increases, the EPs also stop being circular for a single CLC layer [37,38].

E. The influence of CLC sublayers pitches

Now let us investigate the influence of sublayer pitch changes onto the system's reflection spectra. We present the CLC sublayer helix pitches in the forms $p_i = (-1)^{i+1} p_0 + x$ ($p_0 > 0, i = 1,2$), that is, we assume that the helix pitches of the right-hand CLC sublayers increase and those of the left-hand CLC sublayers decrease (by modulo) and we consider the influence of changes of x on the reflection spectra. Figure 13

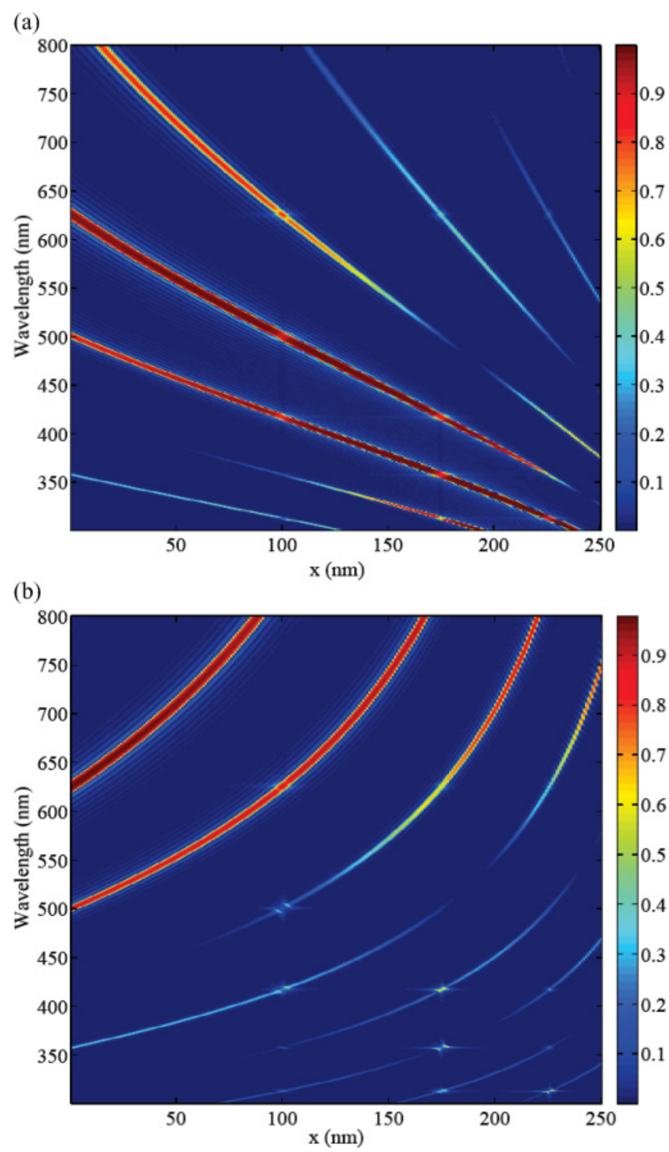

FIG. 13. (Color online) The density plot of the reflection spectra as a function of the pitches change x. The incident light has the (a) LCP and (b) the RCP. $s = 50$, $d_1 = d_2 = 420$ nm, $\alpha = 1$.

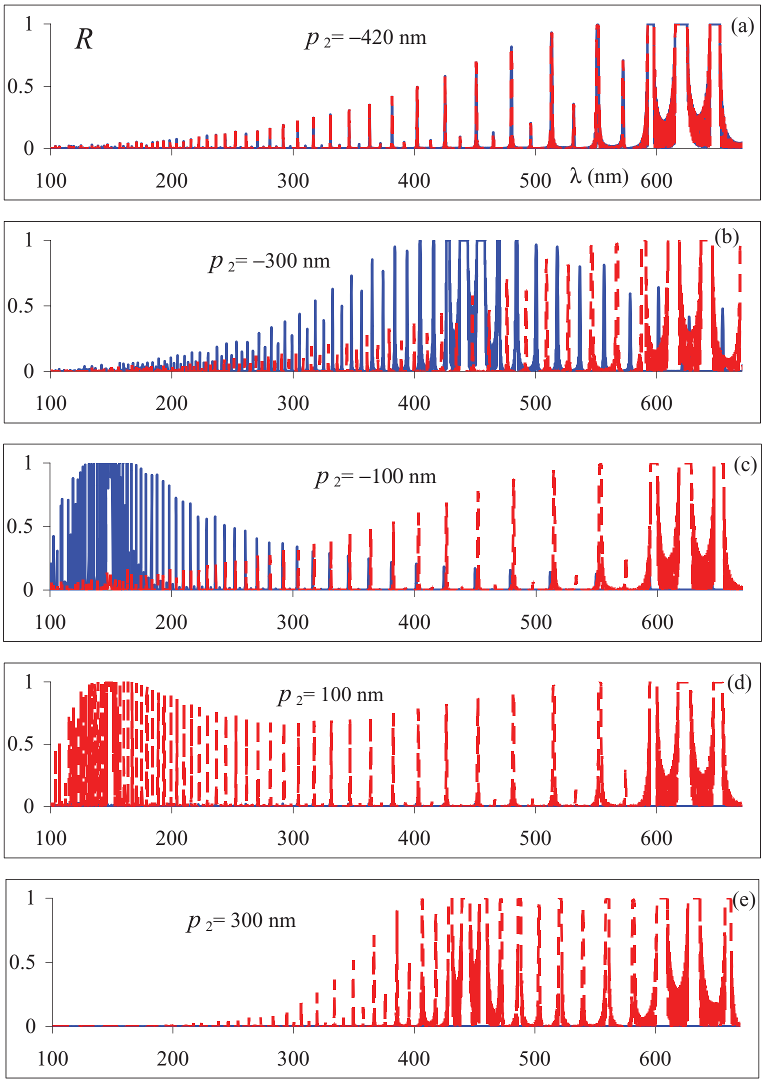

FIG. 14. (Color online) The reflection spectra of R for various p_2. The incident light has the RCP [the red (light gray) dashed lines] and LCP [the blue (dark gray) solid lines]. $p_1 = 420$ nm, $d_1 = 2500$ nm, $s = 50$, $\alpha = 1$.

presents the density plot of the reflection spectra as a function of x. The incident light has LCP [Fig. 13(a)], and RCP [Fig. 13(b)]. For $|p_1| \neq |p_2|$, the reflection spectra become polarization sensitive, as if two diffraction patterns are formed: the first of them is the result of the diffraction of the incidence light with the LCP at the equidistant layers with left-hand CLC sublayers, and the second is the result of the diffraction of the incidence light with the RCP at the equidistant layers with the right-hand CLC sublayers. Therefore, the principal diffraction reflection maxima for the incident light with the LCP shift to the short wave region, and those with the RCP shift to the long wave region.

Now we consider another situation. We assume that the helix pitch of the right-hand CLC sublayers p_1 is constant and that of the left-hand CLC sublayers p_2 changes. Figure 14 presents the spectra for various p_2. The incident light has RCP [the red (light gray) dashed lines] and LCP [the blue (dark gray) solid lines]. If the magnitude of p_2 decreases, the diffraction pattern of the incident light with the RCP (diffracting at equidistant CLC sublayers with a constant right-hand helix) practically remains unchanged, and the diffraction pattern principal maxima for the incident light with the LCP (diffracting at equidistant CLC sublayers with a constant left-hand helix) are shifted to the short wave region. For positive p_2, that is, when the two CLC sublayers are right hand both diffraction patterns are observed for the incident light with the RCP, and the incident light with the LCP transmits practically completely.

IV. CONCLUSIONS

In conclusion, we investigated reflection spectra peculiarities of a stack of right- and left-handed chiral photonic crystal layers. These studies provide important insights into self-assembled photonic crystal applications for adaptive microscale optical devices (consisting of a stack of right and left-handed cholesteric liquid crystal layers). We showed that the system has multiple PBGs. This property of the subject system can find application, in particular, in the display industry. Conventional side-by-side red, green, and blue color filters waste two-thirds of incident light. The alternative of stacking cyan, magenta, and yellow layers is also challenging—a 10% loss per layer compounds to nearly 50% overall. The subject system can give three colors without any loss. Taking into account the possibility of tuning the width, number, and frequency location of these regions by external

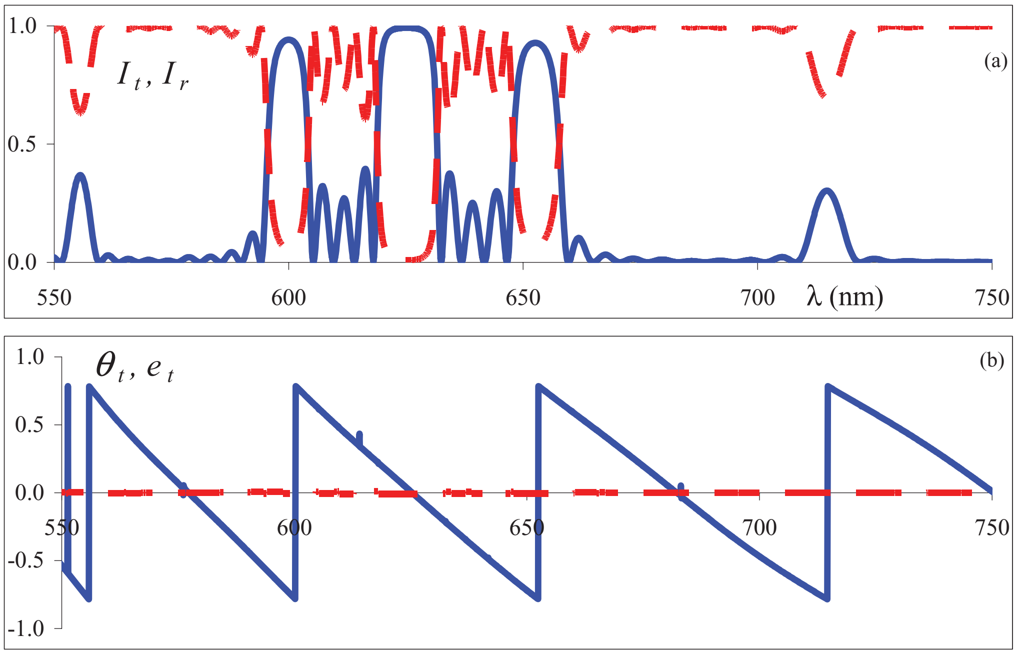

FIG. 15. (Color online) The spectra of (a) the intensities: I_t is the transmitted one [the red (light gray) dashed line] and I_r is the reflected one [the blue (dark gray) solid line], (b) is the azimuth θ_t [the blue (dark gray) solid line] and the ellipticity e_t [the red (light gray) dashed line] of the polarization ellipses of the completely polarized component of the transmitted one, and for the reflected wave we have $e_r \approx e_t$, $\theta_r \approx \theta_t$. The incident light is completely nonpolarized ($P = 0$). $s = 10$, $d_1 = d_2 = 2520$ nm, $\alpha = 1$.

(electric, magnetic, mechanical, thermal, or light) fields, or changing the internal structure of the system, it seems that such systems can have perspectives.

Now let us go to the details.

To describe the interaction of partially polarized quasi-monochromatic light with optical systems usually Muller matrix formalism is used [23,39]. To solve the reflection-transmission problem one usually assumes that

$$\vec{S}_t = \hat{M}_t \vec{S}_i, \quad \vec{S}_r = \hat{M}_r \vec{S}_i, \tag{10}$$

where $\vec{S}_i, \vec{S}_t, \vec{S}_r$ – 4×1 are Stocks' vector columns of the incident and transmitted and reflected waves, respectively: $\vec{S}_i = I\{1,\ P\cos(2\Phi_i)\cos(2\Psi_i),\ P\cos(2\Phi_i)\sin(2\Psi_i),\ P\sin(2\Phi_i)\}$, I is the incident wave total intensity, Ψ_i is the azimuth, and Φ_i is the ellipticity angle of the polarization ellipse of the completely polarized component of the incident wave. P is the incident wave polarization degree, $\vec{S}_{r,t} = (S_0^{r,t}, S_1^{r,t}, S_2^{r,t}, S_3^{r,t})^T$ and $S_0^{r,t}, S_1^{r,t}, S_2^{r,t}, S_3^{r,t}$ are Stocks' parameters of the reflected and transmitted waves, respectively, and $\hat{M}_t, \hat{M}_r$ are Müller's 4×4 matrices of the transmitted and reflected waves, respectively.

According to the well-known rules, one can obtain Müller's matrices from the corresponding 2×2 reflection and transmission matrices [23]. The intensities of the transmitted and reflected waves are defined from the equation

$$I_{t,r} = S_0^{t,r}. \tag{11}$$

The azimuths $\theta_{t,r}$ and the ellipticity angles $\varepsilon_{t,r}$ of the polarization ellipses of the completely polarized component of the transmitted and reflected waves are defined from the conditions

$$\begin{aligned} \theta_{t,r} &= \frac{1}{2}\mathrm{arctg}\left(\frac{S_2^{t,r}}{S_1^{t,r}}\right), \\ \varepsilon_{t,r} &= \frac{1}{2}\arcsin\left(\frac{S_3^{t,r}}{S_1^{t,r} + S_2^{t,r} + S_3^{t,r}}\right), \end{aligned} \tag{12}$$

and the ellipticities $e_{r,t}$ are defined from the equation

$$e_{t,r} = tg(\varepsilon_{t,r}). \tag{13}$$

In Fig. 15(a) the spectra of the intensities of I_t the transmitted [the red (light gray) dashed line] and I_r reflected [the blue (dark gray) solid line] waves are presented. Figure 15(b) presents the spectra of azimuth θ_t [the blue (dark gray) solid line] and the ellipticity e_t [the red (light gray) dashed line] of the polarization ellipses of the completely polarized component of the transmitted wave, and for the reflected wave we have $e_r \approx e_t, \theta_r \approx \theta_t$. The incident light is completely nonpolarized ($P = 0$). As it is seen from the figure, the reflected and transmitted waves are completely polarized (linearly) with a monotonously changing azimuth.

The considered system can have also applications as tunable optical filters or mirrors, etc. The subject system can be used for obtaining a 100% polarized radiation from a nonpolarized one without any loss.

[1] E. Nader and Z. Richard W., Eds., *Metamaterials: Physics and Engineering Explorations* (Wiley-IEEE, New York, 2006), p. 440.

[2] S. A. Ramakrishna and T. M. Grzegorczyk, *Physics and Applications of Negative Refractive Index Materials* (Taylor & Francis Group, New York, 2009).

[3] W. Cai and V. Shalaev, *Optical Metamaterials* (Springer, New York, 2010).
[4] J. Joannopoulos, R. Meade, and J. Winn, *Photonic Crystals* (Princeton University Press, Princeton, NJ, 1995).
[5] K. Sakoda, *Optical Properties of Photonic Crystals* (Springer, Berlin, 2001).
[6] S. G. Johnson and J. Joannopoulos, *Photonic Crystals: The Road from Theory to Practice* (Kluwer, Boston, MA, 2002).
[7] C. M. Soukoulis (Ed.), *Photonic Crystals and Light Localization in the 21st Century*, NATO Science Series C: Vol. 563 (Kluwer Publ., Dordrecht, The Netherlands, 2001), p. 616.
[8] N. Y. Ha, Y. Takanishi, K. Ishikawa, and H. Takezoe, Opt. Express **15**, 1024 (2007).
[9] N. Y. Ha, Y. Ohtsuka, S. M. Jeong, S. Nishimura, G. Suzaki, Y. Takanishi, K. Ishikawa, and H. Takezoe, Nat. Mat. **7**, 43 (2008).
[10] E. M. Nascimento, I. N. de Oliveira, and M. L. Lyra, J. Appl. Phys. **104**, 103511 (2008).
[11] E. M. Nascimento, F. M. Zanetti, M. L. Lyra, and I. N. de Oliveira, Phys. Rev. E. **81**, 031713 (2010).
[12] N. Y. Ha, S. M. Jeong, S. Nishimura, and H. Takezoe, Adv. Matter **22**, 1617 (2010).
[13] Z. He, Z. Ye, Q. Cui, J. Zhu, H. Gao, Y. Ling, H. Cui, J. Lu, X. Gao, and Y. Su, Opt. Commun. **284**, 4022 (2011).
[14] A. H. Gevorgyan, Phys. Rev. E **83**, 011702 (2011).
[15] A. A. Gevorgyan, K. V. Papoyan, and O. V. Pikichyan, Opt. Spectrosc. **88**, 586 (2000).
[16] M. Mitov and N. Dessaud, Nat. Mat. **5**, 361 (2006).
[17] M. Mitov and N. Dessaud, Liq. Cryst. **34**, 183 (2007).
[18] Y. Takanishi, Y. Ohtsuka, G. Suzaki, S. Nishimara, and H. Takazoe, Opt. Express. **18**, 12909 (2010).
[19] H. Sarkissian, B. Ya. Zeldovich, and N. V. Tabiryan, Opt. Lett. **31**, 1678 (2006).
[20] J. A. Reyes and A. Lakhtakia, Opt. Commun. **270**, 51 (2007).
[21] G. A. Vardanyan and A. A. Gevorgyan, Crystallogr. Rep. **42**, 663 (1997).
[22] A. A. Gevorgyan, Opt. Spectrosc. **89**, 631 (2000).
[23] R. M. A. Azzam and N. M. Bashara, *Ellipsometry and Polarized Light* (North-Holland, New York, 1977).
[24] C. Oldano, Phys. Rev. A **31**, 1014 (1985).
[25] K. Rokushima and J. Yamakita, J. Opt. Soc. Am. **73**, 901 (1983).
[26] F. Wang and A. Lakhtakia, Opt. Commun. **235**, 133 (2004).
[27] I. Abdulhalim, L. Benguigui, and R. Weil, J. Phys. (France) **46**, 815 (1985).
[28] M. Z. Arutyunyan, A. A. Gevorgyan, and G. A. Vardanyan, J. Opt. Technol. **74**, 236 (2007).
[29] V. A. Belyakov and V. D. Dmitrienko, Sov. Phys. Solid State **15**, 1811 (1974).
[30] V. D. Dmitrienko and V. A. Belyakov, Sov. Phys. Solid State **15**, 2365 (1974).
[31] A. Lakhtakia and W. S. Weiglhofer, Microwave Opt. Technol. **12**, 245 (1996).
[32] J. A. Polo and A. Lakhtakia, Microwave Opt. Technol. Lett. **35**, 397 (2002).
[33] H. Wohler, M. Fritsch, G. Haas, and D. A. Mlynski, J. Opt. Soc. Am. A **8**, 536 (1991).
[34] K. Robbie, M. J. Brett, and A. Lakhtakia, Nature (London) **384**, 616 (1996).
[35] I. J. Hodgkinson, Q. H. Wu, B. Knight, A. Lakhtakia, and K. Robbie, Appl. Opt. **39**, 642 (2000).
[36] S.-C. Jeng, S.-J. Hwang, Y.-H. Hung, and S.-C. Chen, Opt. Express **18**, 22572 (2010).
[37] A. H. Gevorgyan, Opt. Spectrosc. **92**, 207 (2002).
[38] A. H. Gevorgyan, M. Z. Harutyunyan, A. Kocharian, and G. A. Vardanyan, Mol. Cryst. Liq. Cryst. **432**, 69 (2005).
[39] H. Muller, J. Opt. Soc. Am. **38**, 661 (1948).